



Pediatric focal calvarial lesions: an illustrated review

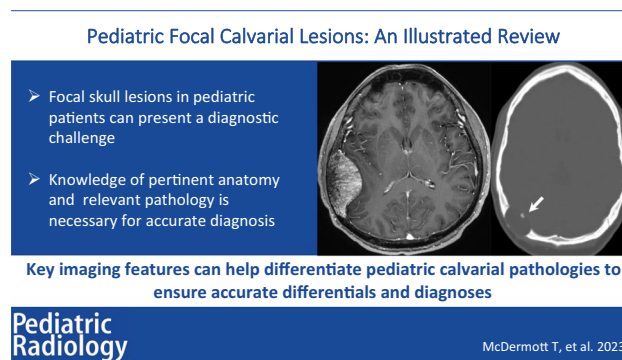
Tyler McDermott¹ · Mohammad Amarnah¹ · Yutaka Sato¹ · Pankaj Watal² · Vijapura Charmi³ · Michaelangelo Fuortes¹ · Sami Faruqi¹ · T. Shawn Sato¹

Received: 20 July 2023 / Revised: 13 October 2023 / Accepted: 16 October 2023 / Published online: 15 November 2023
© The Author(s), under exclusive licence to Springer-Verlag GmbH Germany, part of Springer Nature 2023

Abstract

Focal skull lesions in children can be diagnostically challenging with a wide variety of potential etiologies. Understanding the diverse pathologies and recognizing their associated clinical and imaging characteristics is crucial for accurate diagnosis and appropriate treatment planning. We review pertinent anatomy of the scalp and calvarium and review different pathologies that can present with focal skull lesions in pediatric patients. These include neoplastic, non-neoplastic tumor-like, congenital, post traumatic, and vascular-associated etiologies. We review the key clinical and imaging features associated with these pathologies and present teaching points to help make the correct diagnosis. It is important for radiologists to be aware of the common and rare etiologies of skull lesions as well as the clinical and imaging characteristics which can be used to develop an accurate differential to ensure a timely diagnosis and initiate appropriate management.

Graphical abstract



Keywords Skull lesions · Pediatrics · Calvarium anatomy

✉ T. Shawn Sato
shawn-sato@uiowa.edu

¹ Department of Radiology,
University of Iowa Hospitals and Clinics,
Iowa City, IA, USA

² Department of Radiology,
Nemours Children's Health,
Orlando, FL, USA

³ Department of Radiology,
University of Cincinnati College of Medicine,
Cincinnati, OH, USA

Introduction

Pediatric skull lesions can be a diagnostic dilemma requiring careful evaluation for accurate diagnosis. Their etiologies can run the gamut from benign to malignant and congenital to acquired. It is important to have a comprehensive differential as well as a fundamental understanding of the underlying calvarial anatomy to make an accurate diagnosis.

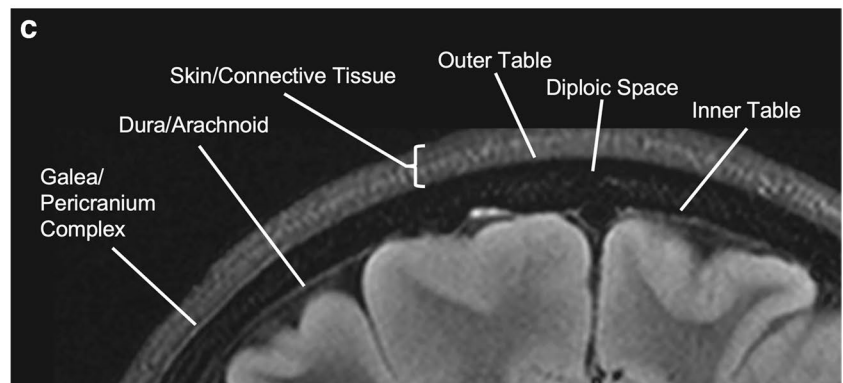
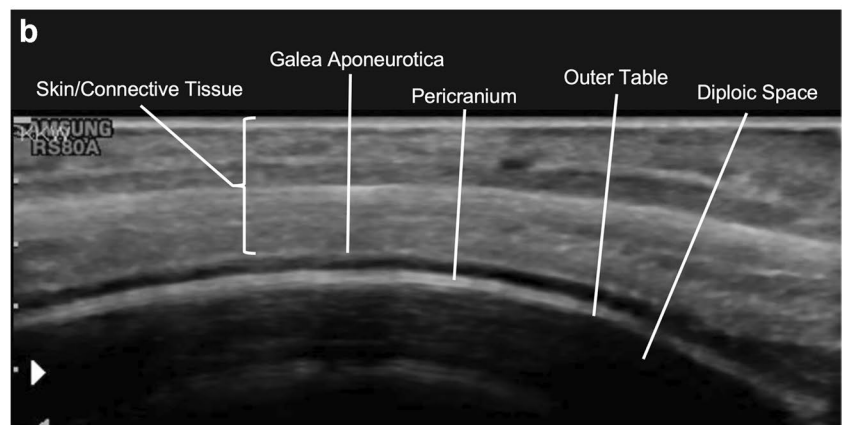
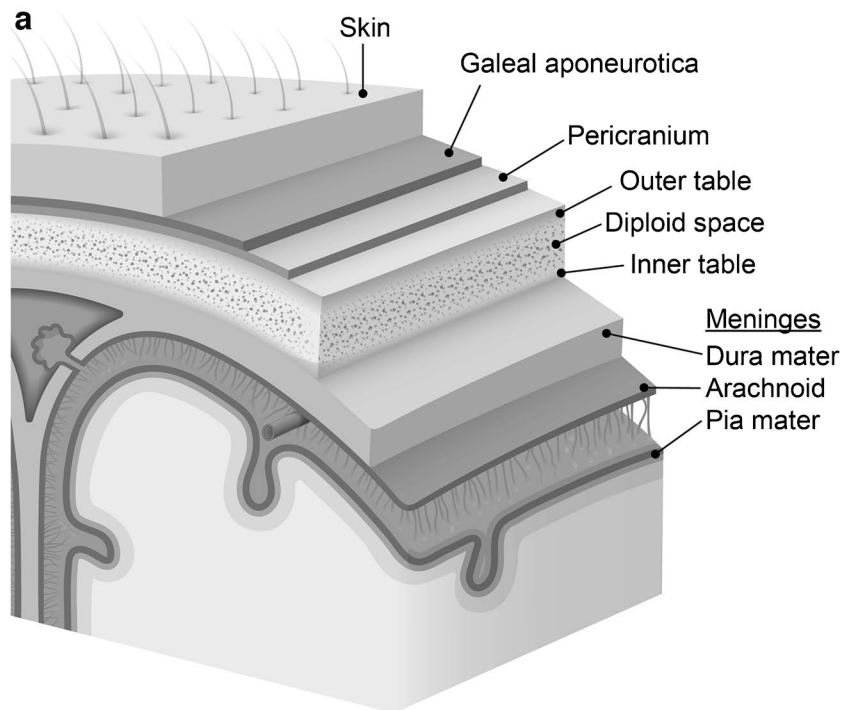
Anatomy

The skull is composed of three osseous components: the calvarium (which is the most cephalad portion of the axial skeleton and protects the brain), the facial bones, and the skull base.

The scalp consists of the soft tissues that cover the calvarium and from superficial to deep consists of the skin, connective tissue, galeal aponeurotica (a continuation of the occipitofrontalis muscles which serves as an anchor for the overlying connective tissue), a layer of loose connective tissue, and the pericranium, a dense connective tissue layer that

adheres tightly to the underlying bone and provides blood supply to the calvarium [1]. Calvarial bones are made of two layers of cancellous bones, the inner table and outer table, surrounding the bone marrow or diploic space. The inner table is lined by the meninges which include the dura, arachnoid, and pia mater (Fig. 1). Familiarity with this anatomy is

Fig. 1 Annotated (a) illustration, (b) transverse ultrasound, and (c) coronal T2 FLAIR MR image of pertinent anatomic structures of the skull and scalp



essential for accurate interpretation and assessment of focal skull lesions.

Neoplastic lesions

Langerhans cell histiocytosis/eosinophilic granuloma

Langerhans cell histiocytosis (LCH) is a multisystemic disorder characterized by abnormal proliferation of Langerhans cells in various tissues. Osseous lesions may be solitary or multifocal, often involving the skull, although can be seen throughout the skeleton. LCH is mostly seen in children ages 5–15 years with a male predominance. Osseous lesions can be asymptomatic, or present with swelling and pain. Other symptoms may include medically refractory otorrhea, and polyps or granular tissue in the external auditory canal [2, 3].

Radiographs and CTs demonstrate a round sharply defined lytic skull defect centered in the diploic space with differential involvement of the inner and outer table resulting in the typical “beveled edge” or “punched out” appearance without bony expansion (Fig. 2) [3–10]. Periosteal reaction is rare in the skull [11]. Healing lesions may demonstrate marginal sclerosis or occasionally a central bony sequestrum. Post contrast CT and MRI often show avidly enhancing inflammatory soft tissue at the edge of the lytic skull lesion which may demonstrate extradural or extracranial extension [3–10]. The well-defined edge of the lytic defect can help differentiate LCH from the permeative defects often seen with metastatic disease [12]. LCH lesions may demonstrate fluid–fluid levels on MRI. Other lesions that may demonstrate fluid–fluid levels include aneurysmal bone cysts, cephalohematomas, and neuroblastoma metastases [13, 14].

Metastatic disease

In children, metastatic disease to the calvarium is most commonly due to neuroblastoma, although it can be seen with other malignancies such as Ewing sarcoma and rhabdomyosarcoma.

Neuroblastoma is a malignant tumor of the sympathetic nervous system and is the most common extracranial solid malignant tumor in childhood. More than 90% of neuroblastoma cases are diagnosed in children ≤ 5 years of age. The skull lesions are often asymptomatic but may present with painful swelling. Involvement of the orbital bone and skull base can result in proptosis with periorbital ecchymosis termed “raccoon eyes” [5–9, 15, 16].

Metastatic neuroblastoma involvement of the skull can produce several patterns of involvement including apparent widening of sutures, lytic defects, diffusely thickened bones, and “hair-on-end” periosteal reaction. The widening

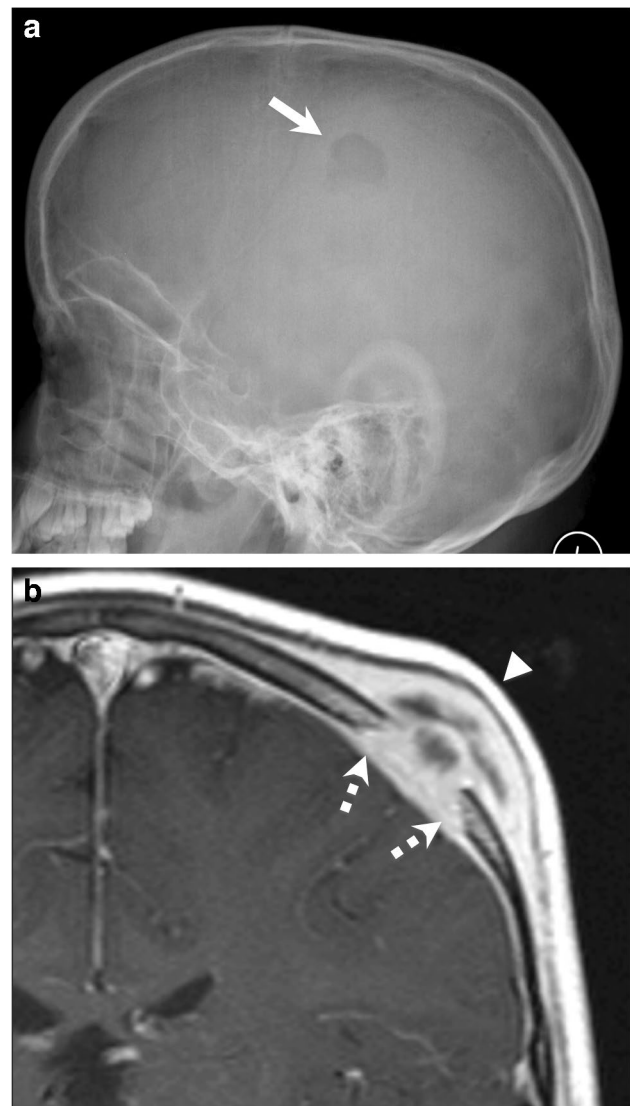


Fig. 2 Eight-year-old male with Langerhans cell histiocytosis. **a** Lateral skull radiograph demonstrates a solitary “punched out” lytic skull lesion (*arrow*) without sclerosis at edge. **b** Coronal post contrast T1 MR image demonstrates the lytic lesion with asymmetric involvement of the inner table relative to the outer table creating the “beveled edge” appearance (*dotted arrow*) with associated dural enhancement and extracranial soft tissue extension and inflammatory changes (*arrowhead*)

of sutures associated with metastatic neuroblastoma is secondary to metastatic infiltration of the suture by tumor and appears less uniform than the sutural separation seen with increased intracranial pressure [5–9, 17]. Radiographic and CT imaging can demonstrate solitary or multifocal lesions with expansion of the diploic space and aggressive imaging features including a wide zone of transition and periosteal reaction, with or without bony destruction which can project through the inner and outer tables of the skull. MRI can demonstrate an enhancing mass centered in the diploic space that can involve both the inner and outer table with associated diffusion restriction (Fig. 3) [5–9, 17].

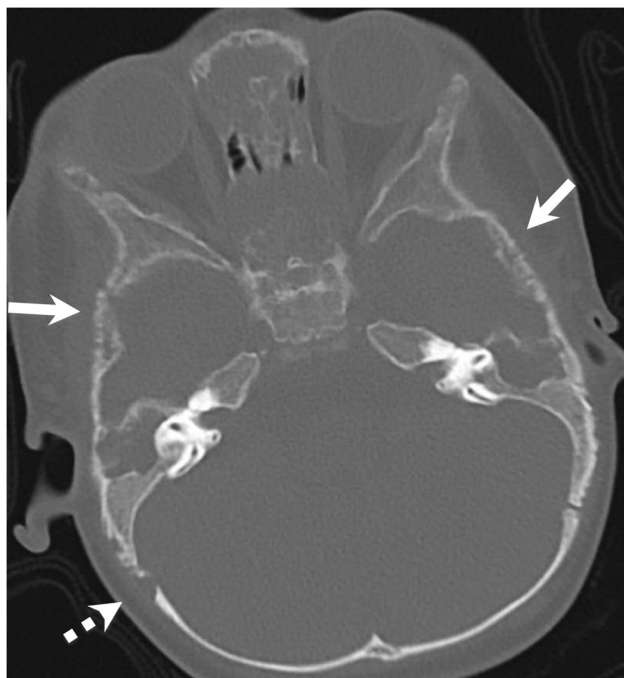


Fig. 3 Seven-year-old male with known neuroblastoma. Axial non-contrast CT on bone windows shows extensive moth-eaten appearance of the temporal bones (*arrows*) and orbits consistent with metastatic involvement. Also, note the widening of the right lambdoid suture (*dotted arrow*)

Chloroma

Chloroma (also known as myeloid sarcoma or granulocytic sarcoma) is a solid extramedullary tumor composed of immature granulocytes in patients with myeloproliferative disorders, such as acute myeloid leukemia (AML). It is twice as common in children compared to adults and can occur in almost any tissue throughout the body. Extramedullary involvement is a defining feature of chloromas, and bones are often involved. It is postulated that leukemic cells from the marrow travel via the Haversian canals and accumulate in the periosteum. Orbital and cranial involvement are common [18–20].

Imaging findings of chloromas can be variable depending on tissues involved. Findings of osseous chloromas include a mixed lytic and sclerotic lesion with permeative bone destruction and periostitis, often with an adjacent soft tissue mass (Fig. 4). Post contrast MRI often demonstrates soft tissue enhancement with associated diffusion restriction. A soft tissue mass may be present even with normal adjacent cortex [18].

Primary bone sarcomas

While osteosarcoma is more common than Ewing sarcoma in pediatric patients, calvarial involvement is more

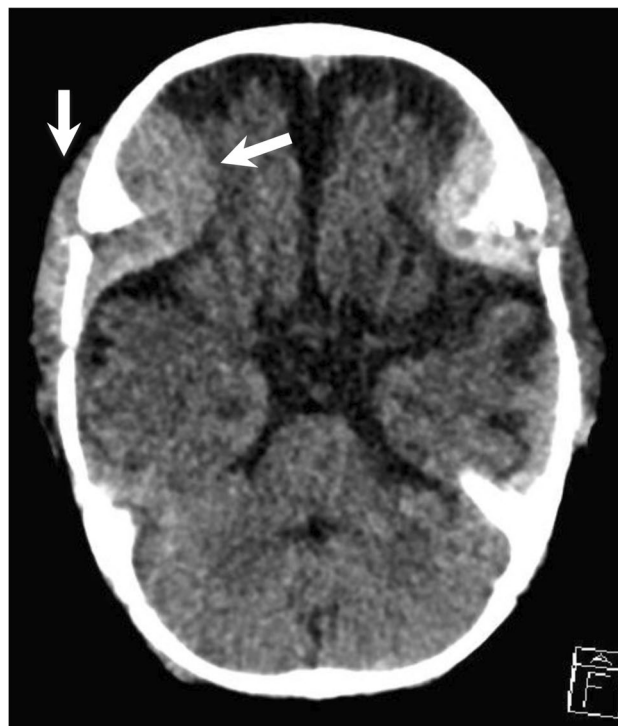


Fig. 4 Eight-month-old male with known refractory erythroid acute myeloid leukemia, presented with fussiness and proptosis. Axial non-contrast CT demonstrates soft tissue masses centered at the calvarium with intra- and extracranial extension (*arrows*) consistent with chloromas

commonly seen with Ewing sarcoma (with metastatic Ewing sarcoma being more common than primary disease) [8, 9, 21].

Patients with calvarial Ewing sarcoma typically present with a rapidly growing head bulge often associated with pain, most commonly involving the frontal and parietal bones. Plain film and CT typically demonstrate a permeative lytic lesion with destructive erosive changes and aggressive periosteal reaction. The outer table involvement is more common than inner table involvement. The onion peel appearance seen at other locations with Ewing sarcoma is rarely seen in the skull. Calvarial lesions are often associated with a large soft tissue mass which is typically iso- to hypointense on T1-weighted imaging, iso- to hyperintense on T2-weighted imaging with heterogeneous enhancement on post contrast MRI imaging (Fig. 5) [8, 9, 22].

Non-neoplastic tumor like

Cranial fasciitis

Cranial fasciitis is a rare, reactive non-neoplastic fibroblastic mass found almost exclusively in young children (<6

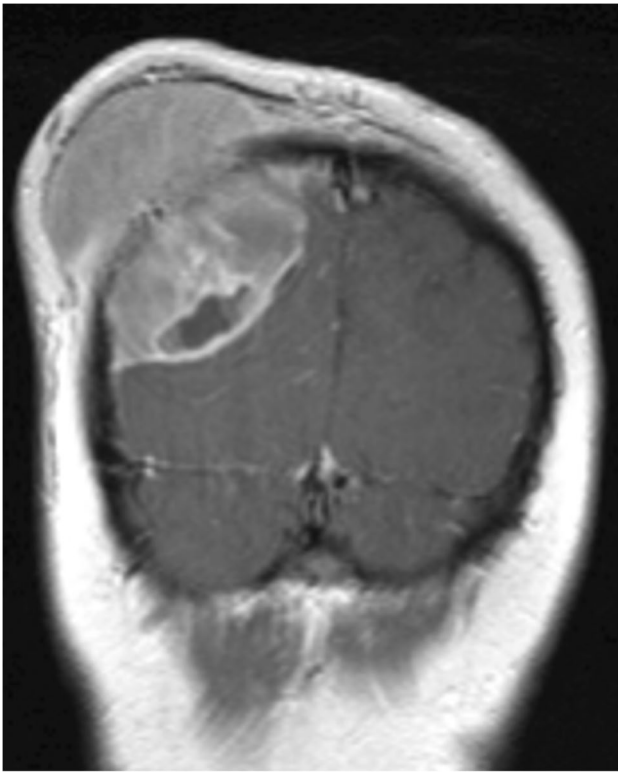
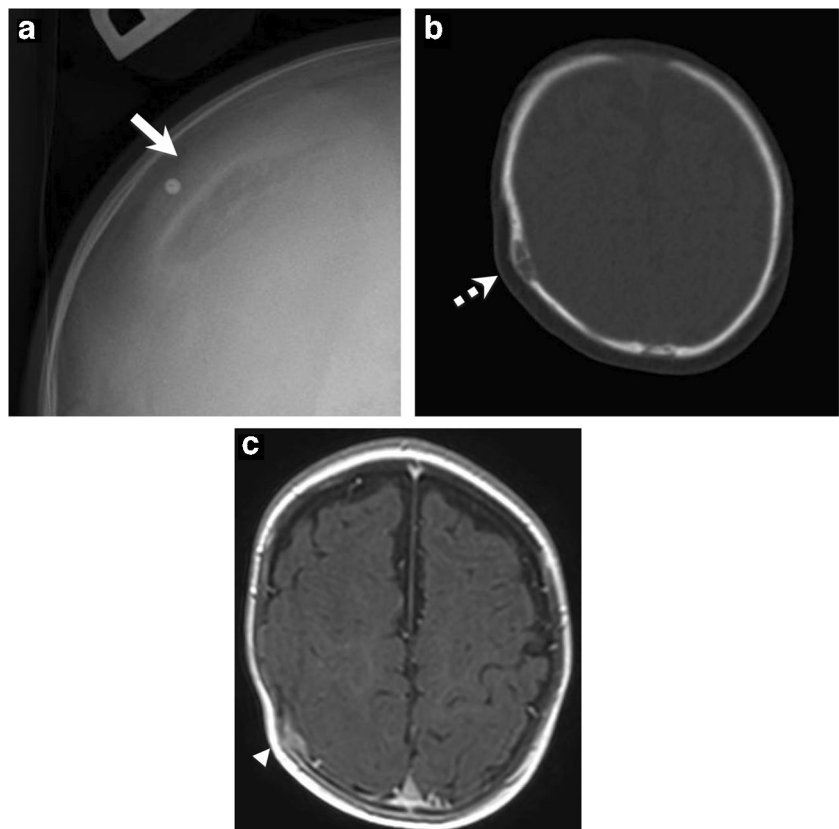


Fig. 5 Thirteen-year-old male with primary calvarial Ewing sarcoma. Coronal T1-weighted post contrast MR image demonstrates an avidly enhancing destructive mass centered in the calvarium with both intra- and extracranial extension

Fig. 6 Six-month-old male with cranial fasciitis. **a** Frontal skull radiograph demonstrates a well-defined lytic lesion (*arrow*) in the right parietal bone at site of lesion (externally marked). **b** Axial non-contrast CT shows a lytic lesion (*dotted arrow*) centered at the diploic space. **c** Axial post contrast T1 MR image demonstrates the lesion with avid enhancement (*arrowhead*) without diffusion restriction (not shown)



years old). Patients often present with a single palpable rapidly enlarging scalp mass originating from the deep fascial layers and the periosteal layer of the calvarium. Typically, the outer table of the skull is involved with an adjacent subcutaneous soft tissue mass. Surgical excision is the definitive therapy, with recurrence being rare [23, 24].

Radiographic and CT images show a well-defined lytic defect in the calvarium associated with a soft tissue mass (Fig. 6). MRI shows an isointense lesion relative to gray matter on both T1 and T2 sequences, with avid enhancement and associated dural enhancement without diffusion restriction [23, 24].

Fibrous dysplasia

Fibrous dysplasia is a focal proliferation of fibrous tissue interspersed with immature osteoid matrix resulting in expansion of the diploic space. The diagnosis is often incidental; however, the most typical presentation is a growing nontender mass often associated with symptoms related to mass effect from impingement on adjacent nerves. Fibrous dysplasia can involve any bone and may be monostotic or polyostotic. While typically sporadic, there are associations with McCune-Albright syndrome (precocious puberty, polyostotic fibrous dysplasia, and café au lait spots) and Mazabraud syndrome (fibrous dysplasia and intramuscular myxomas). Calvarial fibrous dysplasia favors the frontal and temporal bones and can cross suture lines [3–9].

Radiographic and CT imaging demonstrates an intradiploic lesion resulting in expansion of the outer table with preserved inner table, resulting in thickened bones with “ground glass” appearance secondary to the fibrous matrix (Fig. 7). MRI is often unnecessary in diagnosis, with the appearance being variable depending on composition of fibrous tissue versus mineralized matrix. Post contrast images show heterogeneous enhancement which can mimic malignancies; lack of diffusion restriction can help differentiate from malignancies [3–9].

Congenital

Parietal foramina

Parietal foramina are benign abnormalities of calvarial ossification and appear as a single or paired parietal skull defect with intact dura, pericranium, and scalp (Fig. 8). These may range from a few millimeters to several centimeters in size, and often decrease in size with age and rarely necessitating treatment. These foramina can transmit emissary veins draining into the superior sagittal sinus. Parietal foramina can be familial with an autosomal dominant inheritance pattern [5].

Dermoid cysts

Dermoids are congenital slow-growing ectodermal inclusion cysts that contain squamous epithelium with dermal appendages such as sebaceous glands, hair follicles, and sweat glands. They tend to develop in the midline occipital region and periorbital region or along suture lines/near anterior fontanelle. Dermoids are usually discovered during childhood or in young adults. Clinically, they appear as non-tender, slowly expanding masses [3–10].



Fig. 7 Ten-year-old presented with decreased vision in the right eye. Coronal non-contrast CT demonstrates thick bones with “ground-glass” appearance involving the sphenoid bone consistent with fibrous dysplasia. Note the reduced size of the right optic canal (arrow) compared to the left (dotted arrow). Patient subsequently underwent a surgical decompression of the optic canal

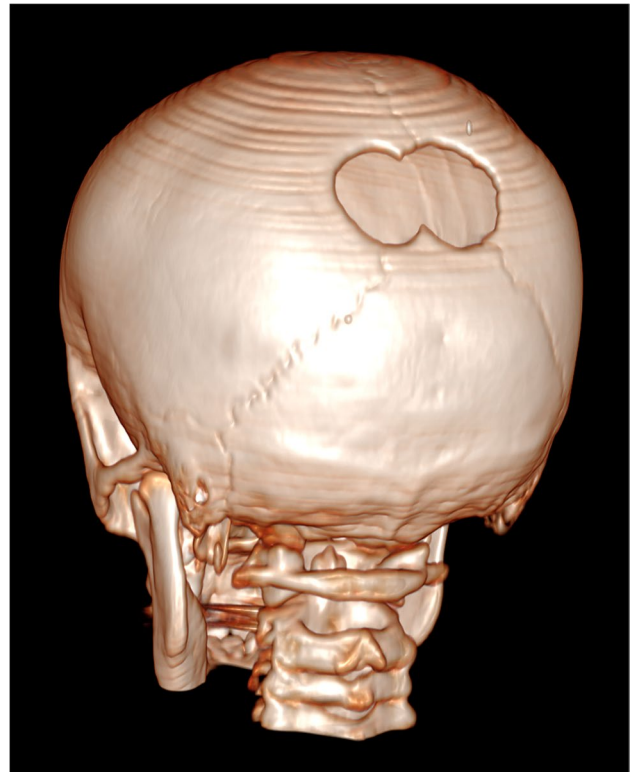


Fig. 8 Ten-year-old male who was noted to have a midline depression at the parieto-occipital junction of his scalp. 3D-rendered posterior projection CT image reveals a large well-margined bilobed defect centered around the sagittal suture most consistent with enlarged bilateral parietal foramina

Radiographs and CT demonstrate an oval well-circumscribed osteolytic lesion, which tends to expand both the inner and outer table, often with sclerotic margins and a soft tissue component, and which can extend intracranially or into the adjacent soft tissue. Intracranial/extracranial extension of the soft tissue is more commonly seen in dermoid cysts than epidermoid cysts. The soft tissue component of dermoid cysts has fat attenuation (Fig. 9) and can occasionally have internal calcifications. MRI frequently shows T1 hyperintense signal within the soft tissue component corresponding to the macroscopic fat, with the signal being suppressed on the fat-saturated images. There is usually no enhancement or mild rim enhancement on post contrast images. Occipital and nasofrontal dermoid may be associated with sinus tracts and intracranial extension [3–10, 25].

Epidermoid cyst

Epidermoids are ectodermal inclusion cysts which are lined by squamous epithelium and may contain cholesterol and keratin. Patients often present with a painless, slowly expanding mass. Epidermoid cysts tend to occur in the third or fourth

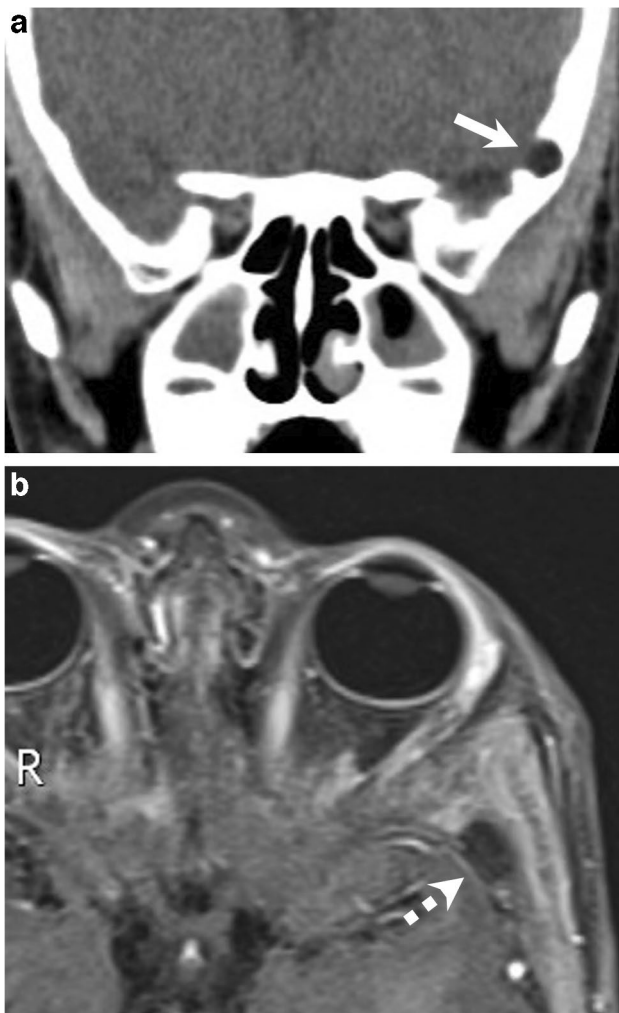
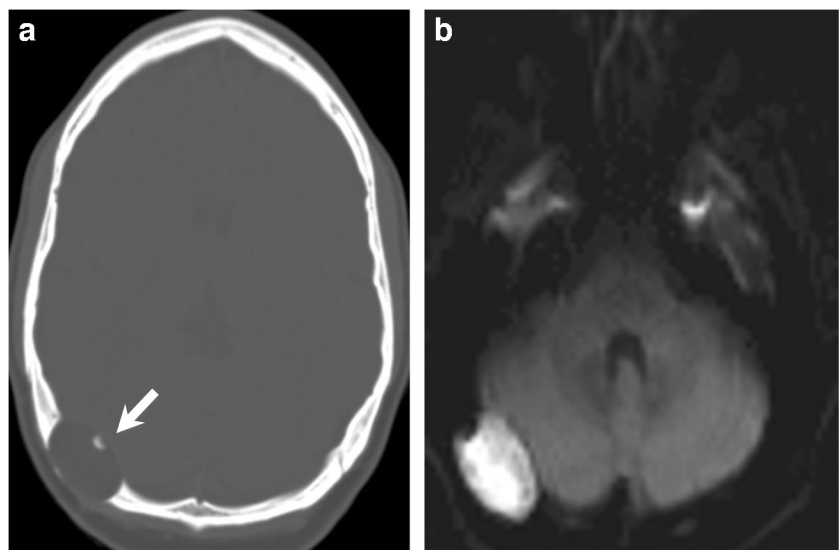


Fig. 9 Thirteen-year-old female with incidentally found calvarial dermoid. **a** Coronal non-contrast CT demonstrates a circumscribed extra-axial fat attenuation lesion extending across the inner table of left temporal bone (*arrow*) with adjacent focal marrow expansion. **b** Axial post contrast T1 fat saturation MR image shows a fat-saturated lesion with no enhancement (*dotted arrow*)

Fig. 10 Fifteen-year-old female with painless palpable lump. **a** Axial non-contrast CT demonstrates a circumscribed lytic lesion in the right occipital bone causing expansion of the inner and outer tables (*arrow*). **b** Axial diffusion-weighted MR imaging shows diffusion restriction corresponding to the area of the lytic lesion, consistent with a calvarial epidermoid cyst



decade of life but can be seen at any age. The parietal and frontal bones are most frequently involved [3–10, 25].

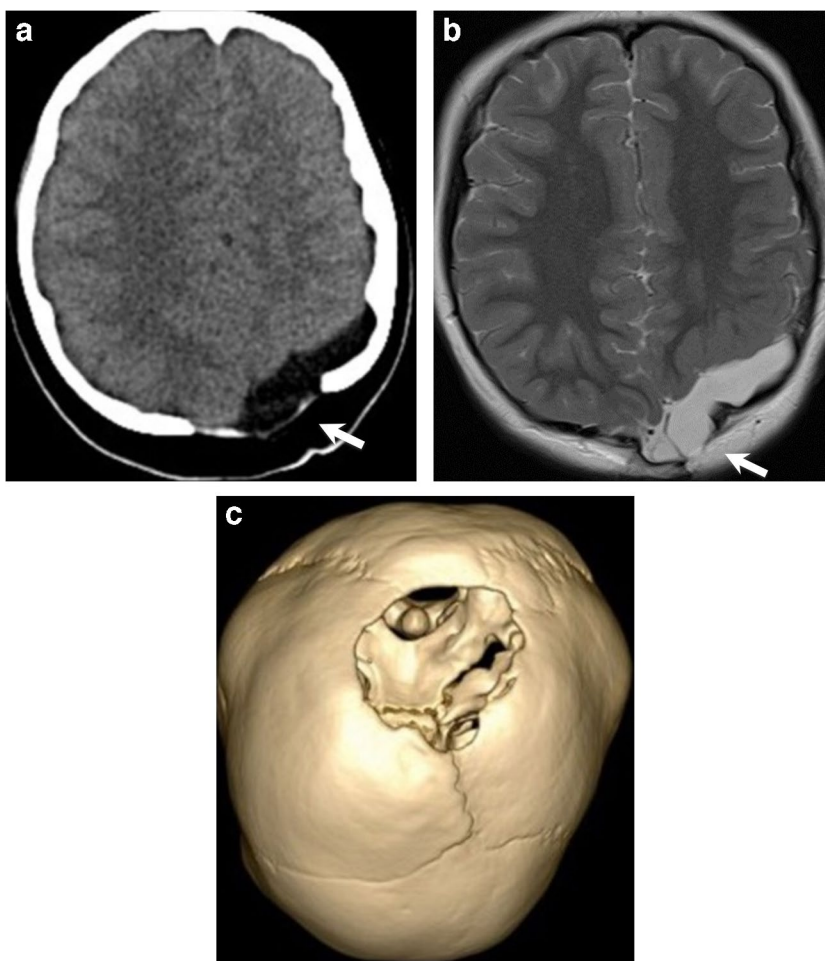
Radiographs and CTs demonstrate well-circumscribed osteolytic lesions centered in the diploic space with smooth sclerotic margins. They often demonstrate adjacent bony expansion immediately adjacent to the lytic lesion with remodeling/scalloping of both the inner and outer tables. This adjacent bony expansion can help differentiate dermoid and epidermoid cysts from LCH where adjacent bony expansion is rare. Sclerosis is also common in dermoid and epidermoid cysts while it is typically not seen in LCH. MRI often demonstrates iso-/hyperintense T2 and variable T1 signal with minimal or no enhancement [3–10, 25]. Epidermoid cysts are more likely than dermoids to restrict diffusion (Fig. 10), but up to 45% of dermoid cysts may restrict diffusion as well [26].

Aplasia cutis congenita

Aplasia cutis congenita is a rare congenital skin defect which can be associated with an underlying skull defect in approximately 20% of patients. Depending on size of defect, clinical courses can vary; smaller lesions may only involve superficial soft tissue and healing spontaneously, while larger lesions may have associated bony defects with exposure of the dura and venous sinuses which may result in hemorrhage, venous thrombosis, or meningitis. Several congenital anomalies are associated with aplasia cutis congenita including cranial arteriovenous malformations, meningomyelocele, cranial stenosis, porencephaly, leptomeningeal angiomatosis, neural tube defects, and congenital heart disease. Diagnosis is often clinical with a focal ulceration over the skull vertex [5, 9].

Calvarial defects in aplasia cutis congenita are well margined, involving both inner and outer tables without bony remodeling. Imaging with CT and MRI can be used to

Fig. 11 Eight-month-old with scalp lesion at birth. **a** Axial non-contrast CT and **(b)** axial T2-weighted MR images show a defect in the left parietal skull (*arrow*) with underlying extra-axial fluid collection deep to the defect. **c** 3D reconstructed image demonstrates skull defect. Clinical and imaging findings consistent with aplasia cutis congenita



visualize the underlying calvarial defect, as well as to look for additional congenital anomalies (Fig. 11) [5, 9].

Atretic parietal cephalocele

Atretic parietal cephalocele (meningocele/encephalocele) is a congenital lesion containing meninges and fibrous tissue with or without brain tissue, thought to represent involution of a true cephalocele. A meningocele involves herniation of the meninges only, while a meningoencephalocele involves herniated meninges and brain tissue. Patients have a subcutaneous soft tissue mass with intracranial extension through a well-margined calvarial defect. The scalp masses can range in size from 10 to 35 mm. Other characteristic radiographic features include a cerebrospinal fluid (CSF) tract and vertical falcine vein directed towards the subcutaneous soft tissue mass with a “spinning-top” configuration of the tentorial incisura (Fig. 12). A fibrous stalk can also be seen that connects the soft tissue mass to the dura mater. A focal

fenestration may be seen in the superior sagittal sinus. MRI is frequently used to visualize contents within the herniation and identify the extent of the brain abnormalities [3, 5, 9, 27].

Post traumatic lesions

Cephalohematoma

Cephalohematomas are traumatic subperiosteal hematomas caused by a disruption of the superficial veins along the pericranium that communicate with veins in the diploic space. They most commonly occur following prolonged instrumental deliveries [3, 5, 9].

Cephalohematomas appear as well-demarcated crescentic-shaped collections along the outer table of the skull. They are limited by cranial suture lines and do not cross the midline. Most will resorb within the first month of life; however, 3–5%

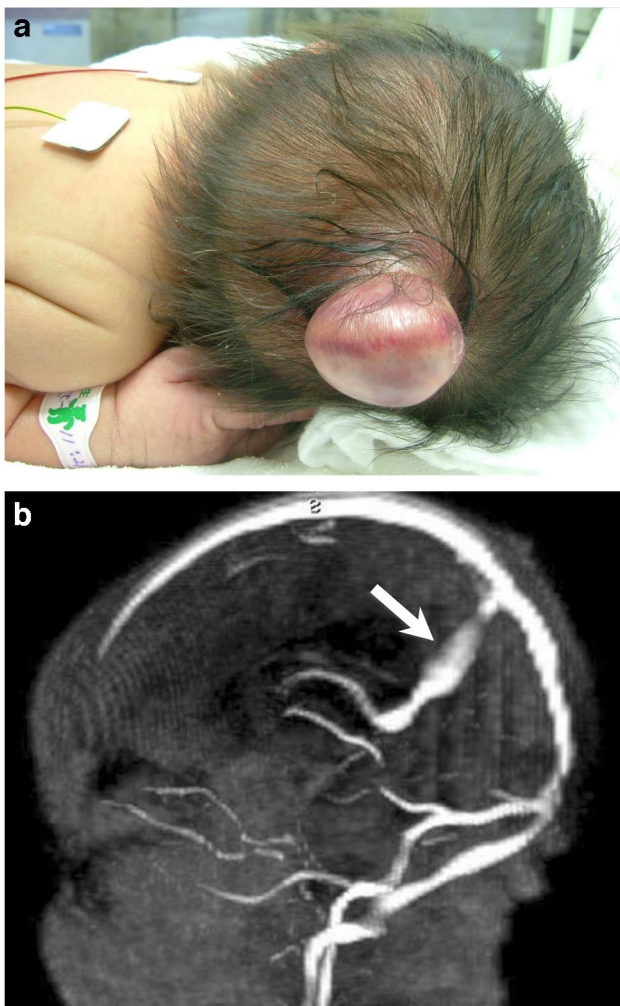


Fig. 12 **a** Newborn with occipital mass seen at birth. **b** Sagittal post contrast MR venogram status post repair shows a persistent primitive falx vein (*arrow*), as is characteristic for an atretic cephalocele

will persist resulting in calcification. Initially the thin rim of elevated periosteum will calcify, then as the hematoma is resorbed, the rim thickens and gets incorporated into the outer table of the skull, which may result in a thickened palpable area of the calvarium (Fig. 13). Most cases of cephalohematoma are diagnosed based on history and clinical exam, and they rarely require imaging. US is a good initial exam in the acute setting and if needed, MRI may be helpful with the internal fluid demonstrating signal findings consistent with subacute blood products and susceptibility artifacts seen on gradient sequences. CT may also be helpful for preoperative planning in cases of reconstruction [3, 5, 9].

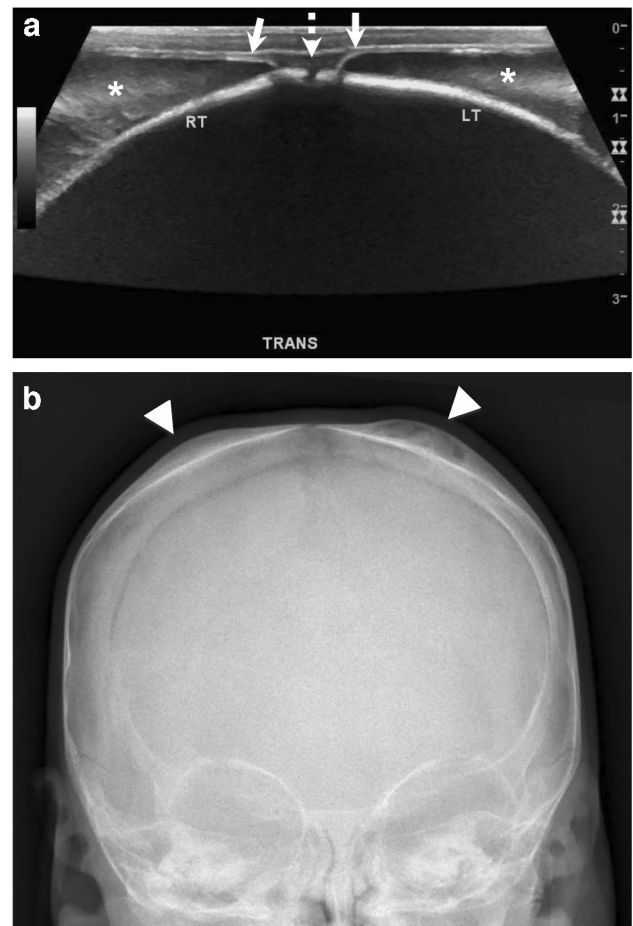
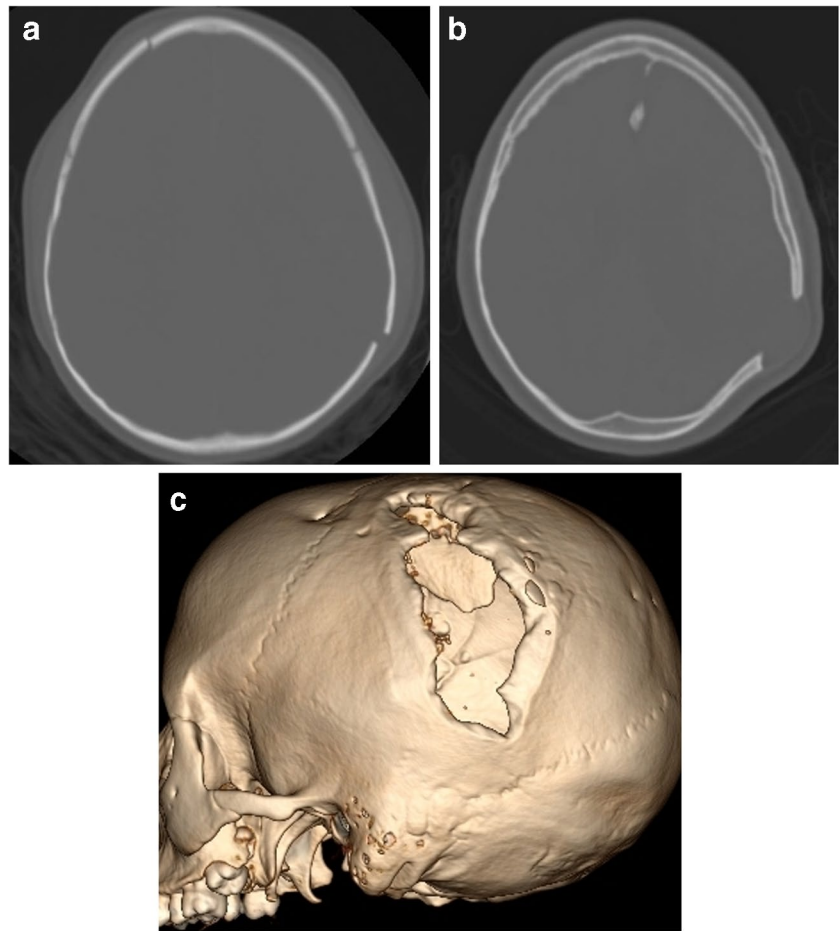


Fig. 13 Two-week-old female following prolonged vacuum and forceps-assisted delivery. **a** Transverse ultrasound over the vertex demonstrates bilateral fluid collections (*asterisks*) in the subperiosteal space, between the pericranium (*arrow*) and the outer table. Note both collections respecting the sagittal suture (*dotted arrow*). **b** Frontal radiograph at 5 months of age demonstrates subsequent calcification of bilateral cephalohematomas (*arrowhead*), with complete incorporation into the outer table on the right, and incomplete incorporation on the left

Leptomeningeal cyst

Leptomeningeal cysts are a complication of pediatric cranial trauma. They almost always occur in patients less than 3 years of age secondary to linear skull fractures which result in a tear of the dura causing the arachnoid membrane and possible brain tissue to invaginate into the fracture line. CSF pulsations tend to widen the fracture line resulting in an ovoid well-margined defect with scalloped margins (Fig. 14) [5, 6].

Fig. 14 Two-year-old female with history of trauma. **a** Initial axial non-contrast CT demonstrates a left parietal skull fracture (as well as a right frontal fracture). **b** Axial non-contrast CT 7 months later demonstrates interval increase in size of left parietal defect. **c** 3D reconstruction image demonstrates irregular elongated defect in the skull with scalloped margins, consistent with leptomeningeal cyst



Vascular-associated lesions

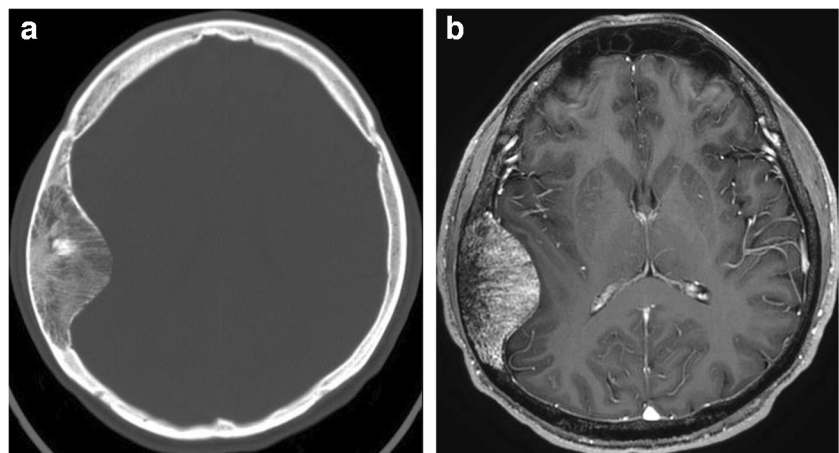
Intraosseous venous malformation

Intraosseous venous malformations (previously called intraosseous hemangiomas) are non-neoplastic slow flow venous anomalies most-commonly seen in craniofacial bones. They are often discovered incidentally, but may

present with pain, swelling, facial paralysis, or hearing loss. They are more common in females and most frequently seen in adults, although they can rarely be seen in children [3–6, 8–10, 28].

Radiographic and CT imaging demonstrates an osteolytic and expansile lesion centered in the diploic space, often displaying a spiculated matrix due to radiating bony trabeculae (Fig. 15). Thickened trabeculae or the “polka-dot” pattern

Fig. 15 Five-year-old male with intraosseous venous malformation. **a** Axial CT demonstrates the characteristic striated pattern due to bony spicules radiating from center to periphery of the lesion. **b** Axial T1 post contrast MR image again shows the striated pattern, with intense enhancement and linear non-enhancing radiating bony spicules



is well described in interosseous venous malformations, and radiologic appearance in typical cases is diagnostic. Tissue confirmation is rarely needed. On MRI, intraosseous venous malformations are hyperintense on T2-weighted imaging with punctate areas of low signal secondary to fibrous tissue or calcifications. Post contrast images demonstrate avid enhancement with non-enhancing septa which become homogeneous on delayed images due to progressive enhancement from slow flow [3–6, 8–10, 28].

Sinus pericranii

Sinus pericranii is a congenital venous anomaly characterized by abnormal communication between the extracranial and intracranial venous structures through diploic varices. This lesion often presents as a well-marginated calvarial defect with an associated cutaneous mass. The soft tissue mass can increase in size with supine positioning due to changes in intracranial pressure. Sinus pericranii is associated with blue rubber bleb nevus syndrome, a rare sporadic syndrome characterized by multifocal venous anomalies [3, 5].

Ultrasound is useful for initial diagnosis, demonstrating flow within the mass communicating to the underlying dural venous sinus (Fig. 16). CT venography can be used to visualize the calvarial defect, with abnormal communication between the dural sinus and the extracranial veins. The imaging appearance of the subcutaneous mass can be variable, as thrombosis is common in these slow flow lesions [3, 5].

Bone infarct

The skull is a relatively uncommon place for bone infarcts, but these can be seen in patients with sickle cell disease. Acute changes are best seen on MRI with non-specific high T2 signal. Sclerosis can be seen later in the disease process on plain film, CT, and MRI. These lesions can be associated with epidural and/or subperiosteal hematomas, which are thought to be secondary to vessel ischemia resulting in wall necrosis and extravasation of blood into the extraosseous space (Fig. 17) [29].

Conclusion

Focal skull lesions in pediatric patients can be challenging for radiologists due to their varied imaging appearances. By integrating clinical information with characteristic imaging findings, radiologists can effectively develop a focused

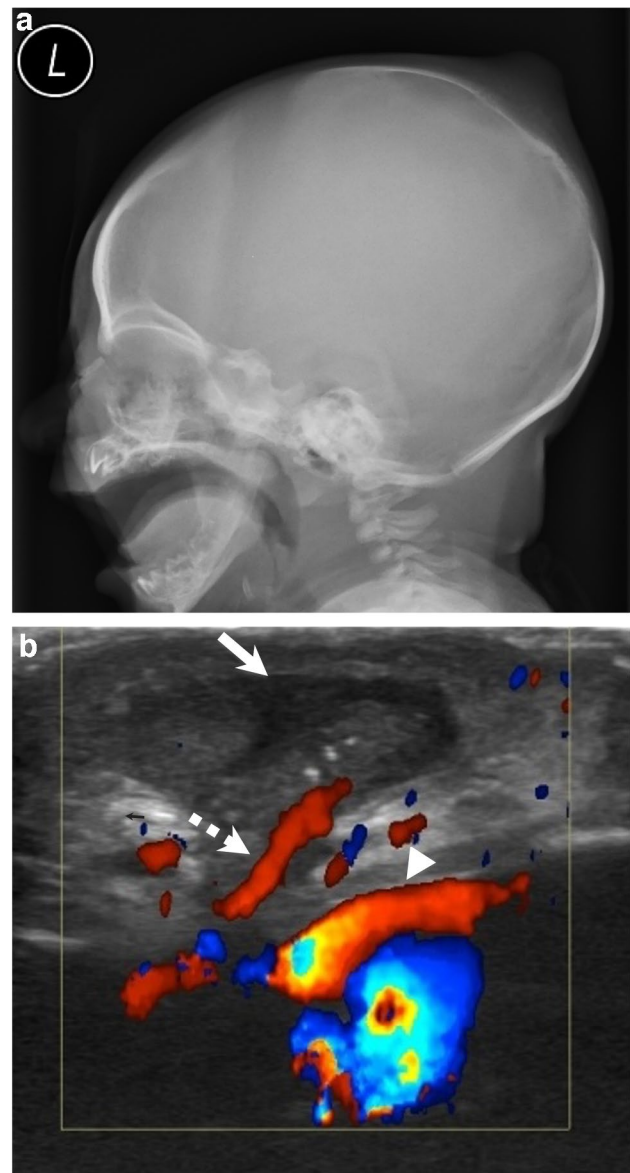


Fig. 16 Fourteen-day-old male with posterior scalp mass. **a** Lateral plain film demonstrates midline soft tissue mass posteriorly. **b** Ultrasound imaging shows a hypoechoic mass (*arrow*) with underlying skull defect and transosseous venous drainage vessel (*dotted arrow*), which connects the mass to the underlying superior sagittal sinus (*arrowhead*), consistent with sinus pericranii

differential diagnosis. Based on the imaging and clinical findings presented in the paper, we have created a flowchart (Fig. 18) to assist in narrowing the differential diagnosis. We hope this will facilitate accurate and efficient management decisions.

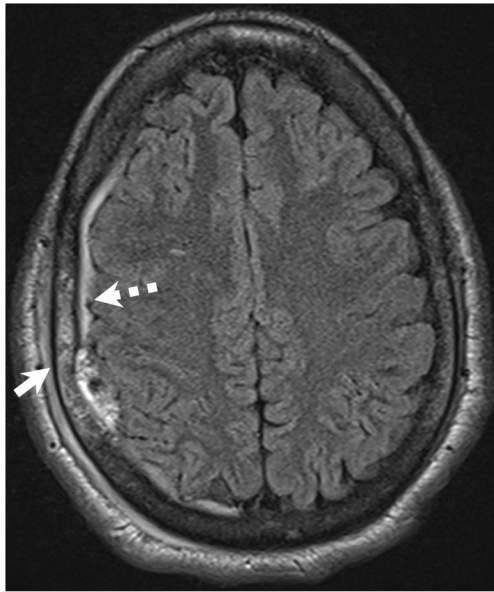


Fig. 17 Seventeen-year-old male with known sickle cell disease presenting with focal tenderness in the right parietal region. Axial FLAIR MR image demonstrates a hyperintense signal in the right parietal bone (*arrow*) consistent with a bone infarct. There is subtle underlying extra axial hyperintense FLAIR signal (*dotted arrow*) consistent with epidural hematoma

Acknowledgements We would like to acknowledge Teresa Ruggle for her valuable contribution to this project in creating the illustration for Fig. 1a.

Author contribution TSS and YS conceived, supervised, and supported the study. All authors contributed in data collection. TM drafted the manuscript and all authors contributed substantially to its revision. TSS takes responsibility for the paper as a whole.

Data Availability The data used to support the findings of this study are included within this article.

Declarations

Ethics approval and consent to participate This is an observational study. The University of Iowa Hospitals and Clinics Research Ethics Committee has confirmed that no ethical approval is required.

Conflicts of interest None

References

1. Sharman AM, Kirmi O, Anslow P (2009) Imaging of the skin, subcutis and galea aponeurotica. *Semin Ultrasound CT MR*. 30:452–64
2. Sliba I, Sidani K, El Fata F et al (2008) Langerhans’ cell histiocytosis of the temporal bone in children. *Int J Pediatr Otorhinolaryngol* 72:775–86

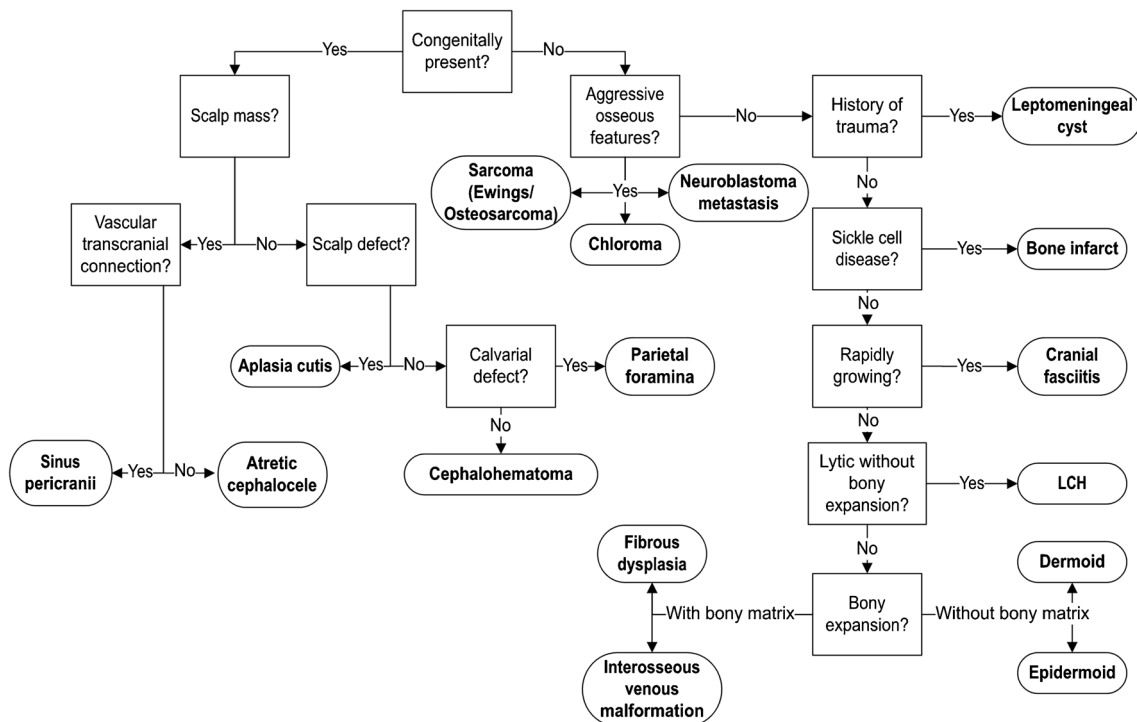


Fig. 18 Flowchart for evaluating focal calvarial lesions in children

3. Morón FE, Morriss MC, Jones JJ, Hunter JV (2004) Lumps and bumps on the head in children: use of CT and MR imaging in solving the clinical diagnostic dilemma. *Radiographics* 24:1655–1674
4. Colas L, Caron S, Cotten A (2015) Skull vault lesions: a review. *AJR Am J Roentgenol*. 205:840–847
5. Khodarahmi I, Alizai H, Chalian M et al (2021) Imaging spectrum of calvarial abnormalities. *Radiographics* 41:1144–1163
6. Willatt JM, Quaghebeur G (2004) Calvarial masses of infants and children. A radiological approach. *Clin Radiol*. 59:474–486
7. Mitra I, Duraiswamy M, Benning J, Joy HM (2016) Imaging of focal calvarial lesions. *Clin Radiol*. 71:389–398
8. Gomez CK, Schiffman SR, Bhatt AA (2018) Radiological review of skull lesions. *Insights Imaging* 9:857–882
9. Choudhary G, Udayasankar U, Saade C et al (2019) A systematic approach in the diagnosis of paediatric skull lesions: what radiologists need to know. *Pol J Radiol* 84:e92–e111
10. Rajakulasingam R, Botchu R, Vemuri VN et al (2020) Skull imaging-radiographs and CT revisited. *Neurol India* 68:732–740
11. Samara A, Nepute J, Lu HC et al (2019) Calvarial Langerhans cell histiocytosis in an adult: typical imaging findings in an atypical age group. *Radiol Case Rep* 14:1478–1482
12. Khung S, Budzik JF, Amzallag-Bellenger E et al (2013) Skeletal involvement in Langerhans cell histiocytosis. *Insights Imaging* 4:569–579
13. Nabavizadeh SA, Zarnow D, Bilaniuk LT (2014) CT and MRI of pediatric skull lesions with fluid-fluid levels. *AJNR Am J Neuroradiol* 35:604–608
14. Matsushita K, Shimono T, Miki Y (2020) Langerhans cell histiocytosis with multiple fluid-fluid levels in the parietal bone. *Magn Reson Med Sci* 19:5–6
15. Moran DE, Donoghue V (2010) Periorbital ecchymosis ('raccoon eyes') as the presenting feature of neuroblastoma. *Pediatr Radiol* 40:1710
16. Papaioannou G, McHugh K (2005) Neuroblastoma in childhood: review and radiological findings. *Cancer Imaging* 5:116–27
17. D'Ambrosio N, Lyo JK, Young RJ et al (2010) Imaging of metastatic CNS neuroblastoma. *AJR Am J Roentgenol* 194:1223–1229
18. Meyer HJ, Beimler M, Borte G et al (2019) Radiological and clinical patterns of myeloid sarcoma. *Radiol Oncol* 53:213–218
19. Almond LM, Charalampakis M, Ford SJ et al (2017) Myeloid sarcoma: presentation, diagnosis, and treatment. *Clin Lymphoma Myeloma Leuk* 17:263–267
20. Guermazi A, Feger C, Rousselot P et al (2002) Granulocytic sarcoma (chloroma): imaging findings in adults and children. *AJR Am J Roentgenol* 178:319–325
21. Vasquez L, Tejada V, Maza I, Mendoza R (2019) Primary osteosarcoma of the skull in teenager. *BMJ Case Rep* 12:e229585
22. Narayanan G, Sreelesh KP, Somanathan T, Soman LV (2016) Ewing's sarcoma of the cranial vault. *J Neurosci Rural Pract* 7:S109–S111
23. Xiang Y, He S, Zhou Z et al (2022) Cranial fasciitis in children: clinicoradiology features and management. *BMC Pediatr* 22:551
24. Alshareef M, Klaphthor G, Alshareef A (2019) Pediatric cranial fasciitis: discussion of cases and systematic review of the literature. *World Neurosurg* 125:e829–e842
25. Yim Y, Moon WJ, An HS et al (2016) Imaging findings of various calvarial bone lesions with a focus on osteolytic lesions. *J Korean Soc Radiol* 74:43–54
26. Serrallach BL, Orman G, Hicks MH et al (2022) Conventional and advanced MR imaging findings in a cohort of pathology-proven dermoid cysts of the pediatric scalp and skull. *Neuroradiol J* 35:497–503
27. Martinez-Lage JF, Sola J, Casas C et al (1992) Atretic cephalocele: the tip of the iceberg. *J Neurosurg* 77:230–5
28. Pati AK, Nayak BB, Choudhury AK, Rout DK (2014) Primary intraosseous venous malformation of nasal bone: a rare case report. *Indian J Plast Surg* 47:423–6
29. Arends S, Coebergh JA, Kerkhoffs JL et al (2011) Severe unilateral headache caused by skull bone infarction with epidural haematoma in a patient with sickle cell disease. *Cephalalgia* 31:1325–1328

Publisher's Note Springer Nature remains neutral with regard to jurisdictional claims in published maps and institutional affiliations.

Springer Nature or its licensor (e.g. a society or other partner) holds exclusive rights to this article under a publishing agreement with the author(s) or other rightsholder(s); author self-archiving of the accepted manuscript version of this article is solely governed by the terms of such publishing agreement and applicable law.